ISSN 1392–1320 MATERIALS SCIENCE (MEDŽIAGOTYRA). Vol. 19, No. 3. 2013

Modeling of Processes in Co-Based Coatings Exposed to Plasma Jet Irradiation

Darya ALONTSEVA [1*], Alexander POGREBNJAK [2], Tatyana KOLESNIKOVA [1], Alyona RUSSAKOVA [3, 4]

[1] *East-Kazakhstan State Technical University, 69 Protazanov St., Ust-Kamenogorsk, 070004, Kazakhstan*
[2] *Sumy State University, 2 Rimsky Korsakov, Sumy, 40007, Ukraine*
[3] *L.M. Gumilev Eurasian National University, 5 Munaitpasov St., Astana, 010008, Kazakhstan*
[4] *Institute of Nuclear Physics NNC RK, 1 Ibragimov St., Almaty, 050032, Kazakhstan*

crossref http://dx.doi.org/10.5755/j01.ms.19.3.1903

Received 17 June 2012; accepted 06 January 2013

The model of microstructure of thick (about 300 μm) plasma detonated Co-based coatings on steel substrates is suggested on the basis of experimental research. Computer simulation of temperature distribution in depth from the surface of coatings under plasma jet irradiation was done; and certain parameters for additional treatment by irradiation were proposed. The irradiation was carried out according to the design conditions. It was established that the roughness of the modified coatings decreased by 2 times, microhardness increased on the average by 25 %. There was established the evolution of the structure and phase composition of the coatings after irradiation, which caused the improvement of their strength.

Keywords: computer simulation, plasma-detonation coatings, structure-phase compositions.

1. INTRODUCTION

The plasma detonation method allows obtaining coatings from high-melting metal powder in air medium. The formation of nanostructures in materials of the coatings applied by this method seems likely, since it is known that especially effective amorphous or nanostructured states are achieved at high heating speeds, high pressure, and short exposure to high temperatures [1]. Due to the high temperatures, at which the coatings are formed, we can expect that the structures formed are thermally stable, in contrast to the nanocomposite films prepared by reactive magnetron sputtering [2–5]. In papers [6, 7] the authors identified several major problems inherent in nanocomposite films prepared by reactive magnetron sputtering. First, it is necessary to achieve their resistance to oxidation, and second, to satisfy the requirement of thermal stability. When the temperature exceeds a threshold value T_c, the material of the film begins to crystallize. This leads to the destruction of the nanostructure and the formation of new crystalline phases, for which reason the nanocomposite films lose their unique properties at $T > T_c$. The thermal stability of plasma-detonation coatings, however, can be due to the formation of crystalline intermetallic compounds in the process of coating deposition, as well as by the increase of their volume fraction in the coating at additional exposure [2–5, 8–10].

The papers [8–10] point out that the intermetallic compounds formed in the Ni-based plasma-detonation coatings improve their corrosion resistance and strength. It is necessary to note that the carbidic strengthening phase in Ni and Co-based alloys at the temperatures of 700 °C – 800 °C coagulates much faster than the intermetallic one, which leads to quick loss of alloy strength [11]. Therefore for work in high temperature areas the alloys with intermetallic hardening are more preferable. Due to considerable depth of the plasma-detonation coating (100 μm – 500 μm) there is no problem of bonding of a high-duty and brittle surface film with the main material with much lower strength and high plasticity. The process of deformation takes place in a consistent structure mode through all the coating and the intermediate layer between the coating and the substrate.

Ni, Cr, and Co are the basic materials for development of solid, corrosion- and wear-resistant coatings [5, 12]. As well as alloys based on Ni, Co-based alloys can have an fcc lattice, which gives a technological advantage in comparison with alloys based on Cr with a bcc lattice. In particular, the alloys with the fcc lattice are better welded, they retain strength at higher temperatures, are less prone to grain increase during heating, and do not lose ductility at low temperatures [12]. The choice of a Co-based alloy coating as the main material of the research is conditioned in the first place by the desire to get the structure of the coating with an fcc lattice, and with the release of intermetallic phases, that is, a structure similar to the previously studied [8–10] structure of the alloy coatings based on Ni. We can assume the precipitation of certain intermetallic phases. The data about existence of a phase with a hexagonal lattice in Co-Cr binary system was first published in [13], the data about its structure was published in [14]. Besides we assumed that the Co-based coatings after duplex treatment can be used for protection of valves and other components working in aggressive environments and in conditions of high friction due to the increased microhardness and reduction of surface roughness. They can be used for the parts of cutting tools, dies, ball bearings, etc.

One of the main problems of plasma detonated thick coatings (100 μm – 500 μm thick) is their porosity, lack of homogeneity on account of poor agglomeration of powder

*Corresponding author. Tel.: +7-7232-252533; fax: +7-7232-267409.
E-mail address: *dalontseva@mail.ru* (D. Alontseva)

particles, high roughness of surface, and low adhesion to substrate. These result in insufficient corrosion and wear resistance of such coatings [4, 5, 15]. To eliminate these drawbacks the coatings may be irradiated by electron beam in vacuum or re-treated by direct current pulse plasma jet on the surface without powder coating in air (duplex treatment).

Practical experience of the use of combined technologies of coating deposition by plasma detonation with the subsequent modification by e-beam or plasma jet allows to claim that the mechanical properties of such coatings of metals and alloys (microhardness, nanohardness, wear resistance, corrosion resistance) are highly desirable [4, 5, 8 – 10]. To scientifically justify the modes of additional irradiation we need to know the structure of coatings before irradiation. There are not enough published TEM-data about the structure-phase composition of coatings deposited by plasma detonation. We need to provide the choice of duplex treatment modes according to the energy of plasma jet, time of action on surface, etc. Therefore we need a correct model of a structure-phase composition of a coating before additional treatment. On the basis of this model we may recommend additional irradiation modes.

The aims of this research are:

1) Developing a model of coating composition on the basis of the experimental data analysis;

2) Estimation of temperature distribution in a two-layer metal sample exposed to a DC pulse plasma jet, depending on irradiation rate intensity, using analytical method and "Diffpack Encounter" licensed application;

3) Establishing structure-phase and mechanical differences in the coatings before and after plasma treatment and giving recommendations for industrial application of such coatings.

2. EXPERIMENTAL DETALS

An "Impulse-6" plasma detonation unit was used to form 150 μm – 300 μm thick protective coatings of powder alloys on stainless Steel 3 substrate (Fe – base, C – 0.25 %, Mn – 0.8 %, Si – 0.37 %, P < 0.045 %). For the coatings we used the AN-35 Co-based powder alloy with additives of Cr (8…32 %); Ni (≤ 3 %), Si (1.7…2.5 %), Fe (≤ 3 %); C (1.3…1.7 %) and W (4…5 %). The powder fractions of the above mentioned composition varied from 56 μm to 260 μm in size. The substrates were (20×30×10) mm^3 steel samples with the surface pre-treated by sandblasting. Plasma-detonation powder coatings were deposited in air using the following modes: the distance from the sample to the plasma jet nozzle edge – 60 mm; sample travel speed – 360 mm/min; pulse frequency – 4 Hz; powder consumption – 21.6 g/min; capacitor bank – 800 μF. The electric current density in a plasma jet can vary from 1 A/cm^2 to 7 A/cm^2; the heat transmission rate in the sample varies in the $q = (0.1…5)\ 10^6$ W/cm^2 depending on the electric current density; the average temperatures of the plasma flow at the nozzle exit of the installation reach the order of several thousand ºC; the average diameter of a plasma jet on a sample is 25 mm; pulse duration of the order of 10 μs [4]. Propane, oxygen and air were used as combustible and orifice gases. Mo was selected as a plasma-jet eroding electrode material.

The coating was deposited and the additional treatment was produced at the Sumy Institute for Surface Modification (Sumy, Ukraine). The modes of additional irradiation by DC pulse plasma jet: power density of plasma jet is 1.9×10^9 W/m^2; pulse duration is 3×10^{-6} sec; pulse frequency is 2.5 Hz. Selecting the power density of the plasma jet to cover the additional processing is based on the results of mathematical modeling of the temperature profile in the double-layer absorbers described in Section 3 of this paper.

Experimental methods of analysis included: Atomic Force Microscopy (AFM) by JSPM-5200 ("JEOL", Japan) and by NT-206 (Belorussia), Transmission Electron Microscopy (TEM) by JEM-2100 ("JEOL", Japan), Scanning Election Microscopy (SEM) by JSM-6390LV ("JEOL", Japan) with Energy Dispersive Spectrometry (EDS) ("Oxford Instruments", Great Britain), X-ray diffraction (XRD) by X'Pert PRO ("PANalytical", the Netherlands). The foils for TEM were prepared by the Ar ion sputter etching method using the Precision Ion Polishing System – M-691 ("Gatan", USA). For a more detailed analysis of the coating, it was mechanically cut off the surface of the substrate to examine the structure at different depth from the coating surface. We used the method of arbitrary secant line to define the volume fraction of phases according to the TEM-images and data [16] and CrystalMaker software to define the parameter of the crystal-lattice according to the TEM-diffraction pattern. Because the thickness of the coatings is from 150 μm to 300 μm, we applied different methods to investigate the structure, element composition and mechanical properties of the coatings at different depths. Thus we investigated different coat layers. Microhardness was measured on the angle laps of coatings by PMT-3 microhardness meter (LOMO, Russia) with an indentation load of 2, 5, and 10 N.

3. MODELLING OF TEMPERATURE PROFILES FOR DC PULSE PLASMA JET MODE SELECTION IN TREATMENT OF Co-BASED PLASMA DETONATION COATINGS

The processes of diffusion and formation of new phases in materials under the influence of DC pulse plasma jet treatment happen very quickly, the temperature being one of the main factors influencing these processes. However the temperature measurement under irradiation conditions is difficult and unreliable. Development of a mathematical model of temperature distribution in a material depending on irradiation parameters makes it possible to assume what structures and phases will form in the material during irradiation (on the basis of the received values of temperature and the known phase diagrams). Based on this model, one can select the parameters of irradiation so as to form sufficiently high temperatures on the boundary of the coating with the substrate to accelerate the diffusion processes in order to improve adhesion of the coating to the substrate. The papers devoted to the development of such a model [17, 18] testify the relevance of this problem, but they do not provide a comprehensive solution.

This scheme (Fig. 1, a) was used at working out the model of the temperature profile distribution in these coatings under irradiation by a plasma jet.

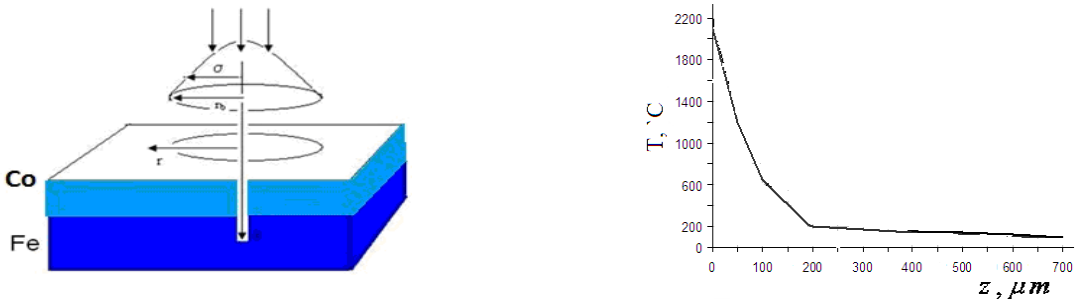

a b

Fig. 1. The geometry of a sample irradiation by a plasma jet. It demonstrates the selection of the cylindrical coordinate system (r, z), jet radius r_b, dispersion of Gaussian distribution σ (a); the diagram of temperature distribution across the depth at the impact of a plasma jet with the power density of $1.9 \cdot 10^9$ W/m^2, (b)

We assumed that the coating might be interpreted as a layer of Co on top of Fe because of the prevailing volume concentration of the Co-based solid solution in the coating, and the square shape of the impulse. The numerical experiment to determine the temperature profiles during irradiation was carried out by mathematical simulation methods. The calculation of the temperature profile was conducted with the "Diffpack Encounter" licensed program. It is assumed that the plasma jet forms a circular spot on the sample. The geometry of the temperature profile in the sample was determined according to the intensity of the energy flow, the time of exposure on the surface and the diameter of the jet. The problem was solved with a periodic current source without consideration of the motion of the source. It was considered in cylindrical coordinates (r, z), where z – the coordinate normal to the surface (Fig. 1, a).

Heat equations (Fourier equations) are given by (1) and (2) for T_1 and T_2, i. e. the functions of the coating and substrate temperatures correspondingly:

$$\rho_1 C_1 \frac{\partial T_1}{\partial t} = \frac{1}{r}\frac{\partial}{\partial r}(\lambda_1 \frac{\partial T_1}{\partial r}) + \frac{\partial}{\partial z}(\lambda_1 \frac{\partial T_1}{\partial z}); \quad (1)$$

$$\rho_2 C_2 \frac{\partial T_2}{\partial t} = \frac{1}{r}\frac{\partial}{\partial r}(\lambda_2 \frac{\partial T_2}{\partial r}) + \frac{\partial}{\partial z}(\lambda_2 \frac{\partial T_2}{\partial z}), \quad (2)$$

where ρ_1 and ρ_2 are the densities, C_1 and C_2 are the specific heats, λ_1 and λ_2 are the thermal conductivity of the coating and the substrate correspondingly, regarded as temperature functions.

Initial conditions:

$$T_1(r,z,0) = T_2(r,z,0) = T_0, \quad (3)$$

where T_0 is the initial temperature of the sample, which was assumed to be 20 °C.

The boundary conditions at infinity for the function of T_1 are of the form:

$$\lim_{r\to\infty} T_1(r,z,t) = T_0. \quad (4)$$

The boundary conditions on the surface of the sample are set by the conditions (5) and (6):

$$\lambda_1 (\frac{\partial T_1}{\partial z})_{z=0} = P(r,t) - \varepsilon\sigma T_1^4, \quad (5)$$

where λ_1 is the thermal conductivity of the coating material, $P(r,t)$ power-to-weight ratio of a flat normal-circular source, switched at the starting time $t = 0$, and acting in the course of time $\tau = \eta/\nu$, where ν is the pulse repetition frequency, and η is the pulse ratio, i. e. the ratio of the pulse duration to the period of repetition), σ is the Stefan-Boltzmann constant, ε is the emissivity factor for the coating material.

$$P(r,t) = \begin{cases} q_{\max} \cdot e^{-\alpha r^2}, t \in (nT, nT+\tau) \\ 0, t \in (nT+\tau(n+1)T) \end{cases}, \quad (6)$$

where an integer index n runs through all values from zero $n \in 0..\infty$, $q_{\max} = kN/\pi$ (N is the beam power, α is the coefficient of concentration associated with the radius of the beam r_b by the correlation α).

The boundary conditions at the boundary between the coating and the substrate $z = h$, where h is the coating thickness, have the form (7) and (8):

$$(T_1)_{z=h} = (T_2)_{z=h}; \quad (7)$$

$$k_1(\frac{\partial T_1}{\partial z})_{z=h} = k_2(\frac{\partial T_2}{\partial z})_{z=h}. \quad (8)$$

The boundary conditions at infinity for the function T_2:

$$\lim_{r\to\infty} T_2(r,z,t) = \lim_{z\to\infty} T_1(r,z,t). \quad (9)$$

The asymptotic solution of the problem has also been considered – the functions

$$T_1(r,z) = \lim_{t\to\infty} T_1(r,z,t)$$

and

$$T_2(r,z) = \lim_{t\to\infty} T_2(r,z,t).$$

Fig. 1, b, presents the corresponding diagram of the function

$$T(r,z) = \begin{cases} T_{1\infty}(r,z), z \in (0,h) \\ T_{2\infty}(r,z), z \in (h,\infty) \end{cases} \quad (10)$$

We assumed the optimal variant of the heating of the upper thin layer of the coating to the Co melting point, respectively (Fig. 4, b), and heating the coating at the entire thickness with the aim of its homogenization. The recommended mode of irradiation: power density of the plasma jet $1 \cdot 10^9$ W/m^2. The irradiation by direct current pulse plasma jet was carried out according to the design conditions.

4. EXPERIMENTAL RESULTS

The roughness of plasma-detonation coatings is very high (see Fig. 2, a). The average value of roughness coefficient R_a is 100 nm. Not fully melted powder particles of the coating are visible on the surface.

The coatings have differences in the phase structure as the depth varies (see Table 1). We noted the reduction of γ-phase parameter *a* in the coatings with depth. In the coating layers that contact the substrate the volume concentration of Fe-based phases rises (Fe is the basic component of the substrate), and the oxides disappear. It was proven by TEM that the base through-thickness layer of plasma detonation coatings is a mixture of crystal-lographically differently oriented nanograins of Co-based solid solution (fcc) with the size of 50 nanometers and lamellas of intermetallic phases up to 50 nanometers long and 5 nm in diameter (Fig. 2, a). Every indexed reflex of intermetallic phases (Fig. 2, b) was tested by the dark field method (see Fig. 2, c). Evidently, it is a $Co_{0.8}Cr_{0.2}$ – phase. The data about existence of a phase with a hexagonal lattice in the Co-Cr binary system was first published in data [11], the data about its structure was published in data [12]. This nanosize phase allows naming strengthening as the highest microhardness of a coating that corresponds to those places where the volume concentration of this phase is largest (Fig. 4). The phase composition of a coating after irradiation according to the design conditions changes, the volume fractions of Co-based solid solution and intermetallic phase increase (see Table 1). Mo appears on the surface of a coating after irradiation under the estimated regimes (Table 1).

a b

Fig. 2. AFM-images of the surface of AN-35 plasma detonation coating before (a) and after irradiation (b)

Table 1. Phase composition of the Co based coating and substrate

Material and the field of analysis	Volume concentration. Chemical formula. Crystal system. Space group. Space group number. Parameters (Å)
AN-35 base powder	20 vol.% – Co-based solid solution, hexagonal (hcp); 70 vol.% – Co-based solid solution, cubic (fcc); 10 vol.% – $CoCr_2O_4$, cubic (fcc), Fm-3m (225), a = 8.2990
Coating AN-35 0 μm – 50 μm from surface	60 vol.% – Co-based solid solution, cubic (fcc), Fm-3m (225), a =3.55 – 3.54 ; 15 vol.% – $Co_{0.8}Cr_{0.2}$, hexagonal, P63/mmc (194), a = 2.52; b = 2.52; c = 4.062; 10 vol.% – $FeCr_2O_4$, cubic (fcc), Fm-3m (225), a = 8.3780; 15 vol.% – CoO, cubic (fcc), Fm-3m (225), a = 4.2200
Coating AN-35 100 μm – 150 μm from surface	50 vol.% – Co-based solid solution, cubic (fcc), Fm-3m (225), a = 3.52 – 3.53; 15 vol.% – $Co_{0.8}Cr_{0.2}$, hexagonal, P63/mmc (194), a = 2.52; b = 2.52 ; c = 4.062; 35 vol.% CoFe, cubic, Pm-3m, 221, a = 2.8570
Coating AN-35 after added irradiation by direct current pulse plasma jet 0 μm – 50 μm from surface	70 vol.% – Co-based solid solution, cubic (fcc), Fm-3m, a = 3.5(4); 20 vol.% – $Co_{0.8}Cr_{0.2}$, hexagonal, P63/mmc, a = 2.52; b = 2,52: c = 4.062; 3 vol.% – $FeCr_2O_4$, cubic (fcc), Fm-3m (225), a = 8.3780; 7 vol.% – Mo, cubic, Pm-3m, a = 3.130 and MoO_2 and MoO_3
St3 substrate	Fe – cubic (bcc), Im-3m (229), a = 2.8662

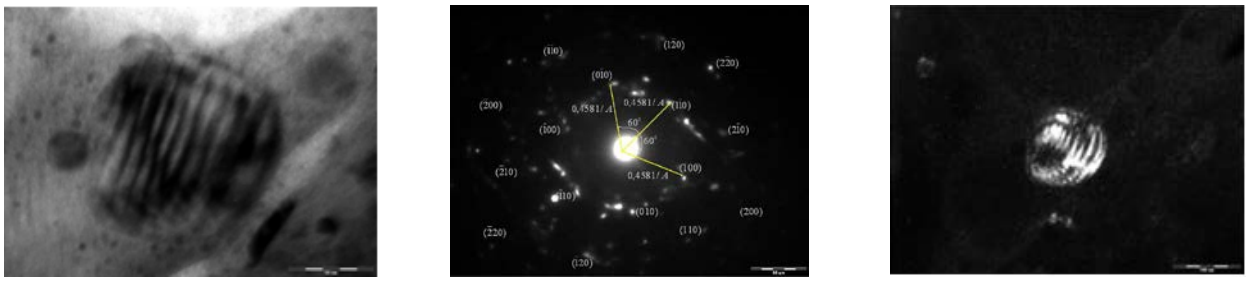

a b c

Fig. 3. TEM – images of AN-35 coating: the $Co_{0.8}Cr_{0.2}$ particle, bright field (a); an electron diffraction pattern of a $Co_{0.8}Cr_{0.2}$ particle, the zone axis is [001](b); the $Co_{0.8}Cr_{0.2}$ particle (dark field) shot in point ref $(0\bar{1}0)$ lex (c)

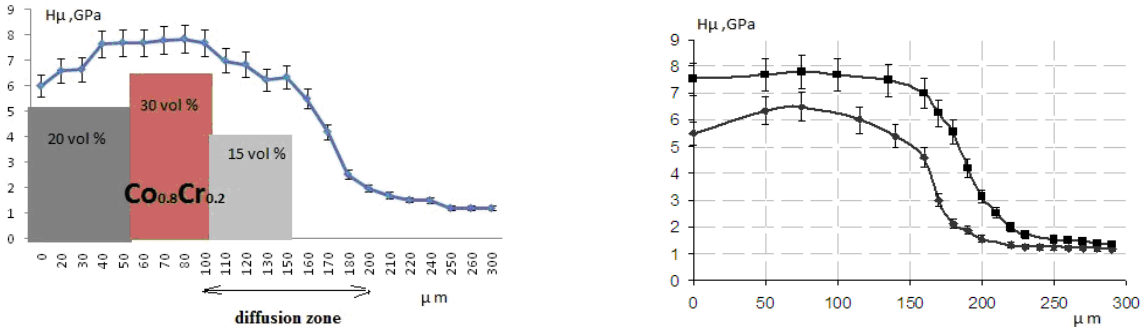

a b

Fig. 4. The distribution of microhardness Hμ in depth from the surface with specification of the intermetallic phase content volume concentration (a); The curves of distribution of microhardness in the coatings with depth before – the lower curve and after irradiation - the upper curve (b)

After further treatment by a plasma jet the adhesion of the coating to the substrate significantly increased, thus making it hard to mechanically cut the coating from the substrate, unlike prior to irradiation. A too thick layer of the steel substrate is taken when cut off. Therefore, Table 1 shows the data obtained only in the analysis of the irradiated coating surface.

Microhardness of a coating increases; the width of the diffuse zone increases (Fig. 4). The roughness decreases (Fig. 2, b) at the expense of melting the coating surface, which corresponds to the specified temperatures at the surface of the coating (Fig. 1, b). The average value of roughness coefficient R_a of a coating after irradiation is 53 nm.

5. DISCUSSION

We assume that the structure-phase state of a coating is defined by the following factors: deformational impact of a plasma jet, the temperature profile distribution in the coating material, and inhomogeneous concentration of elements in a coating. On the basis of the experiment we propose a model of the coating structure (see Fig. 5).

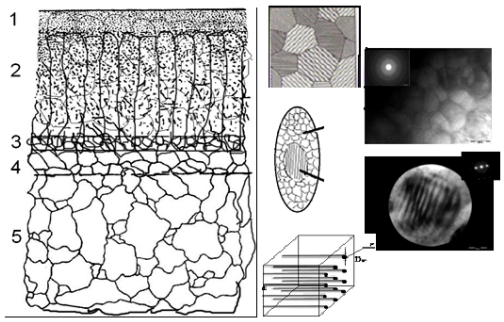

a b

Fig. 5. Model of Co-Cr-based plasma-detonation coatings on a steel substrate (a) with explanatory drawings and images (b), where: 1 – amorphous layer with oxides and carbides; 2 – textured layer (solid Co-based solution with an intermetallic phase) and unmelted particles of coating powder; 3 – intermediate coating layer (coating-substrate) with deformed and broken particles of the coating; 4 – intermediate substrate layer with fine-grained micro-structure; 5 – the substrate with large grains. The strokes show precipitations of lamellas of the intermetallic phase

We consider that the nanocrystalline patterns that are found in AN-35 coating are distinctive for all the coatings deposited by the plasma detonation method, and partially characteristic for the substrate layer next to the coating. One of the reasons is high micro structure defectiveness conditioned by the plasma jet impact action on the surface and steep temperature gradient in the coating, which may lead to considerable coating deformation. As a result, in order to remove the strains in a coating there forms a substructure of nanograins of different crystal lattice orientation with high and continuous disorientation, which is proved by distinctive ring electron-diffraction patterns. When the foils in a goniometer are oriented randomly, the characteristics of polycrystalline features, namely, the changes of their intensiveness on the boundaries, necessary for defining grain edges of diffraction contrast, are absent. We assume that we observe the pattern similar to a fragmented one, with fragment – nanograin – disorientation being analogous to the one of crystal polygonization.

This assumption for the coatings is validated by some diffusion of the peaks and the decrease of their intensiveness on the X-ray diffractograms. The formed structures are stable at room temperature, no reduction of strength properties is observed. We consider that the nano-sized lamellae of $Co_{0.8}Cr_{0.2}$ intermetallic phases are reinforcing, since the microhardness of plasma-detonation coatings varies with depth and correlates with the volume fraction of the phase irradiated electrode and the increase of the width of the diffuse zone in the coating layer contacting the substrate (Fig. 3, b, and Table 1). It is evident that molybdenum penetrates the surface from the Mo electrode. Our results are in good agreement with the data of other authors, who note, firstly, the formation of a polycrystalline matrix of crystallographically disoriented nanograins in films [7] and in protective coatings [19, 20], including plasma-detonation coating [3–5]; secondly, indicate the formation of intermetallic compounds under irradiation of coatings [2–4]; thirdly, notice the radiation-enhanced diffusion in materials with an fcc lattice during irradiation, leading to heating up to the temperatures we specified [21].

6. CONCLUSIONS

The model of structure for plasma-detonation deposited Co-based coatings was developed. Computer

simulation of temperature distribution in depth from the surface of two-layer metals under plasma jet irradiation depending on the irradiation parameters and conditions was carried out. On the basis of calculations the authors offer the irradiation modes that result in melting of a coating surface.

The mechanism of coating improvement was indentified. In general the structure-phase changes are represented by the increase of nanosized intermetallic phase volume concentration and the increase of the width of the diffuse zone in the coating layer contacting the substrate.

REFERENCES

1. **Poate, J. M., Foti, G., Jacobson, D. C.** Surface Modification and Alloying by Laser, Ion, and Electron Beams. N.Y., 1983: 424 p. http://dx.doi.org/10.1007/978-1-4613-3733-1
2. **Ivanov, Yu. F., et al.** Structure and Properties of Coatings Created by Plasma Deposition Technique and Treated by Electron-beam *Russian Physics Journal* 8/2 2009: pp. 402 – 404.
3. **Pogrebnjak, A. D., Il'jashenko, M., et al.** Structure and Properties of Al_2O_3 and Al_2O_3+Cr_2O_3 Coatings Deposited to Steel 3 (0.3 wt% C) Substrate Using Pulsed Detonation Technology *Vacuum* 62 2001: pp. 21 – 26.
4. **Kadyrzhanov, K. K., Komarov, F. F, Pogrebnyak, A. D., et al.** Ion-beam and Ion-plasma Modification of Materials. M., 2005: 640 p.
5. **Misaelides, P., Hatzidimitou, A., Noli, F., et al.** Preparation, Characterization and Corrosion Behavior of Protection Coatings on Stainless Steel Deposited by Plasma Detonation *Surface and Coatings Technology* 180 – 181 2004: pp. 290 – 296.
6. **Musil, J., Dohnal, P., Zeman, P.** Physical Properties and High-temperature Oxidation Resistance of Sputtered Si_3N_4/IVIoN_x Nanocomposite Coatings *Journal of Vacuum Science and Technology B* 23 (4) 2005: pp.1568 – 1575.
7. **Musil, J.** Physical and Mechanical Properties of Hard Nanocomposite Films Prepared by Reactive Magnetron Sputtering. Chapter 10 in the book "Nanostructured Hard Coatings". N.Y., 2005: pp. 407 – 463.
8. **Alontseva, D.** The Study of Using Plasma Technologies for the Deposition of Ni-Cr Based Coatings on Steel Substrate and Modification of Their Properties by Duplex Treatment *Przegląd Elektrotechniczny* 86 (7) 2007: pp. 42 – 44.
9. **Pogrebnjak, A. D., Alontseva, D. L., et al.** The Effect of Electron Beam Fusion on the Structure and Properties of Plasma Jet Sprayed Nickel Alloy Coating *Technical Physics Letters* 30 2004: pp.164 – 167.
10. **Pogrebnjak, A. D., Alontseva, D. L., et al.** Structure and Properties of Coatings on Ni Base Deposited Using a Plasma Jet Before and After Electron a Beam Irradiation *Vacuum* 81 2007: pp. 1243 – 1251.
11. **Hassanein, A. M., Kulsinski, G. N., Wolfer, W. G.** Vaporization and Melting of Materials in Fusion Devices *Journal of Nuclear Materials* 103 – 104 1981: pp. 321 – 326.
12. **Burns, R. M., Bradley, W. W.** Protective Coatings for Metals. N. Y., 1967: 735 p.
13. **Elsea, A. R., Westerman, A. B., Manning, G. K.** The Co-Cr Binary System *Trans. AIME Metals Technology* 180 1949: p. 579.
14. **Jongebreur, R., van Engen, P. G., Buschow, K. H. J.** Magneto-optical Properties of Metallic Ferromagnetic Materials *Journal of Magnetism and Magnetic Materials* 38 1983: pp. 1 – 22.
15. **Celik, E, Ozdemir, I., Avci, E., Tsunekawa, Y.** Corrosion Behavior of Plasma Sprayed Coatings *Surface and Coatings Technology* 193 2005: pp. 297 – 302. http://dx.doi.org/10.1016/j.surfcoat.2004.08.143
16. **Egerton, R.F.** Physical Principles of Electron Microscopy. An Introduction to TEM, SEM and AFM. M., 2010: 304 p.
17. **Pischasov, N. I., Nikolaev, A. V.** Modification of the Structure and Properties of Hard Alloys of WC-Co System by High-current Beams of Charged Particles *Communications of Omsk University* 2 1996: pp. 39 – 43.
18. **Pischasov, N. I., Orlov, P. V.** Simulation of Termal Processes in Inhomogeneous Solids Under High Power Ion Beams *Communications of Omsk University* 1 1997: pp. 35 – 37.
19. **Veprek, S., Argon, A. S.** Mechanical Properties Of Superhard Nanocomposites *Surface and Coatings Technology* 146 – 147 2001: pp. 175 – 182.
20. **Veprek, S., Veprek-Hejman, M. G. J., Kavrankova, P., Prohazka, J.** Different Approaches to Superhard Coatings and Nanocomposites *Thin Solid Films* 476 2005: pp. 1 – 29. http://dx.doi.org/10.1016/j.tsf.2004.10.053
21. **Nolfi, F. V.** Phase Transformation during Irradiation. Ch., 1989: 31 p.